RJC

RASĀYAN *J. Chem.*
Vol. 13 | No. 4 |2123-2132| October - December | 2020
ISSN: 0974-1496 | e-ISSN: 0976-0083 | CODEN: RJCABP
http://www.rasayanjournal.com
http://www.rasayanjournal.co.in

IMPACT OF MOLECULAR INTERACTIONS ON BINARY SOLUTIONS OF 2-PROPANOL WITH METHOXY ANILINE ISOMERS AT DIFFERENT TEMPERATURES

G. V. Gangadhara Rao[1], S. Suriya Shihab[2], D. Das[3] and Shaik. Babu[1,*]
[1]Department of Physics, Koneru Lakshmaiah Education Foundation, Vaddeswaram, Guntur(Dist)-522502, (Andhra Pradesh) India
[2]Department of Physics (Humanities and Social Science), Prakasam Engineering College, Kandukur, Prakasam(Dist)-523105, (Andhra Pradesh) India
[3]Department of Chemistry, Dinhata College, Cooch Behar Panchanan Barma University, Dinhata, 736135, (WestBengal), India
*E-mail: drshaikbabu.physics@gmail.com

ABSTRACT

In this present experiment, thermodynamic fundamental parameters alike density(ρ), speed of sound(U), viscosity(η) were measured for the binary solutions that contain 2-propanol with isomers of 2-methoxy aniline in various concentrations and temperature ranges from 303.15 to 323.15K (5K interval) over ambient atmospheric pressure. The extracted values of excess molar volume(V_m^E), excess isentropic compressibility(K_s^E), deviation in viscosity($\Delta\eta$) and excess Gibbs energy(ΔG^E), which are derived from experimental fundamental values have been correlated with classical polynomial Redlich-Kister function. Furthermore, to reveal specific interactions that are presented in binary solutions, these excess values have been subjected to reduced Redlich-Kister function. Furthermore, the calibration of partial molar volumes($\bar{V}_{1,p,m}$) and ($\bar{V}_{2,p,m}$) composites shows strong interactions in 4-methoxyaniline(1) + 2-propanol(2) than any other composites. Also, this semblance is well substantiated by the FTIR characteristic spectrum of all combinations at various concentrations. Also, the ($\bar{V}_{1,p,m}$) and ($\bar{V}_{2,p,m}$) values of all components have been correlated with Belda equation to test the applicability.

Keywords: Redlich-Kister Functions, Reduced Redlich-Kister Functions, Partial Molar Volumes, Belda Equations and FTIR Spectroscopy.

INTRODUCTION

The molecular interactions in the mixtures of binary liquids play a vital role in applications of recent explorations and, uniquely a great extent to the analysis of thermodynamic fundamental attributes such as volumetric, transport and viscometric. With elegance, these attributes of binary liquid mixtures furnish more precious and unique information that usher to portrays the molecular liquid structures in the binary mixtures. From these fundamental properties, extracted the excess thermodynamic acoustic parameters with accustomed intervals of temperature over ambient atmospheric pressure. Several peers have eclectically computed the thermodynamic excess parameters from fundamental attributes of handful of liquid mixtures, and these attributes have been examined in a concert of specific or non-specific interactions[1-6]. In this investigation monograph, authors reviewed three isomers of methoxy containing aromatic aniline derivatives such as 2-methoxyaniline(2MA), 3-methoxyaniline(3MA) and 4-methoxyaniline(4MA) are mixed individually with 2-propanol(2P) at various concentrations. The three isomers of methoxyaniline and their derivates are mostly used in the prevention of corrosions of iron in oil refinery rigs[7]. On the other hand, 2P greatly used as a solvent in many industrial and pharmaceutical applications leads to a strong association that takes place between dipole-dipole interaction and hydrogen bonding[8-10]. The combination of aromatic aniline group with an alcohol group have much more potential applications and it is more important in both biological systems and as well as industrial, pharmaceutical

http://dx.doi.org/10.31788/ RJC.2020.1345825

systems. The existence of experimental work depicts thermodynamics of multi-component binary liquid mixtures such as 2MA/3MA/4MA(1) + 2P(2) in terms of fundamental parameters with regular intervals of constant temperature ranges from 303.15K to 323.15 K over a constant ambient atmospheric pressure.

EXPERIMENTAL

Material and Methods

In the present sequence, the provenance, CAS number, purity and further purification under chromatography and drying methods of methoxyaniline isomers as well as 2P have been cataloged in Table-1. Furthermore, Table-2 illustrated the purity of 2MA and 2P was quantified by comparison of experimental density, speed of sound and viscosity with literature values. Furthermore, the unexplored density, speed of sound and viscosity values of the 3MA and 4MA are propounded in Table-2.

Table-1: Specification of Provenance, CAS Number, Mass Fraction Purity and Further Purification

Name of the Chemical	Source	CAS Number	Mass Fraction Purity	Further Purification Methods
o-anisidine	TCI Chemicals-India	90-04-0	>98.0%	*GLPC
m-anisidine	TCI Chemicals-India	536-90-3	>98.0%	*GLPC
p-anisidine	TCI Chemicals-India	104-94-9	>98.0%	**Vacuum drying
2-propanol	HiMedia Laboratories, India.	67-63-0	>99.70%	*GLPC

*Gas-Liquid Partition Chromatography carried through Inert gas Ar.
**moisture separation by mass transfer.

General Procedure

The prepared binary mixtures and pure liquids were streamed into glass vials with the help of mass variations of liquids. The vials are covered with airtight lids to prevent evaporation and adsorption of atmospheric moisture. The uncertainty in the final molefraction is estimated to be less than ±0.0001. The binary mixtures of systems such as 2MA(1)+2P(2), 3MA(1)+2P(2) and 4MA(1)+2P(2) were prepared in different concentrations, i.e., molefractions of these systems carried out 12 subsequent values of which, solvation concentration varies from 0 to 1.

Table-2: Physical properties of pure components, 2P, 2MA, 3MAand 4MA with literature at specific temperatures.

Sample	parameter	Expt./Lit.	Temperatures				
			303.15 K	308.15 K	313.15 K	318.15 K	323.15 K
2P	ρ (kg. m^{-3})	Expt.	782.0	772.5	760.2	754.2	747.0
	ρ (kg. m^{-3})	Lit.	781.5[a]	772.0[a]	760.1[a]	754.3[a]	747.0[a]
	U (m.s^{-1})	Expt.	1122.4	1106.0	1088.64	1075.36	1066.0
	U (m.s^{-1})	Lit.	1122.2[a]	1106.2[a]	1088.8[a]	1075.1[a]	1065.8[a]
	η (milli.Pa.sec)	Expt.	1.6540	1.4940	1.3190	1.1832	1.0630
	η (milli.Pa.sec)	Lit.	1.6536[a]	1.4941[a]	1.3195[a]	1.1830[a]	1.0629[a]
2MA	ρ (kg. m^{-3})	Expt.	1091.80	1087.40	1083.80	1080.80	1079.90
	ρ (kg. m^{-3})	Lit.	1091.75[b]	1087.35[b]	1083.78[b]	1080.80[b]	-
	U (m.s^{-1})	Expt.	1595.44	1579.44	1466.32	1454.64	1439.04
	U (m.s^{-1})	Lit.	1595.4[b]	1579.2[b]	1466.3[b]	1454.8[b]	-
	η (milli.Pa.sec)	Expt.	4.9230	4.5124	4.1854	3.8830	3.6832
	η (milli.Pa.sec)	Lit.	4.9225[b]	4.5125[b]	4.1855[b]	3.8825[b]	-
3MA	ρ (kg. m^{-3})	Expt.	1090.25	1087.05	1083.2	1080.05	1070.8
	U (m.s^{-1})	Expt.	1581.2	1550.32	1523.8	1495.4	1475.8
	η (milli.Pa.sec)	Expt.	5.6460	5.1325	4.6344	4.2150	3.9225
4MA	ρ (kg. m^{-3})	Expt.	1089.9	1085.2	1082.6	1079.85	1069.95
	U (m.s^{-1})	Expt.	1555.2	1525.4	1502.8	1480.32	1460.4
	η (milli.Pa.sec)	Expt.	6.3350	5.8560	5.3230	4.7250	4.3450

*The calibrated uncertainties are $Uc(\rho)$=0.036kg.m^{-3}, $U_c(U)$=0.456m.sec^{-1}, $U_c(\eta)$=0.1145milli.Pa.S, $U_c(x_1)$=0.000037, $U_c(T)$=0.01K are carried at ambient atmospheric pressure.
[a] Reference [2], [b] Reference [15]

Analytical Discussion

The densities of pure samples and mixed samples were measured with 10mL specific gravity bottle in high accuracy digital electronic balance supplied by Mettler Toledo, Company-India. The uncertainty weighing balance is approximated to be $\pm 10^{-5}$ kg leads to the accuracy in the densities is estimated to be less than ±0.001 kg m^{-3}. The viscosities of binary liquids were measured with Ostwald's viscometer with the inconstancy of observation was approximated to be less than ±0.001 milli Pa.sec. In each time of observation, the viscometer rinsed with distilled water before calibrating viscosity for all mixtures and solutions. The flow time has been measured with a digital electronic stopwatch with high accuracy of ±0.01s. The speed of sound measurements of samples was performed by using with 2MHz frequency single-crystal ultrasonic interferometer supplied by Nunes, Company-India. The data accuracy in the speed of sound is estimated to be less than ±0.5 ms^{-1}. The parameters of all three systems were encapsulated with regular temperature intervals using a well-stirred circulated water bath furnished by Nunes, Company-India, which has been used to keep constant temperature within the accuracy of ±0.01 K.

RESULTS AND DISCUSSION

The experimentally calibrated parameters of density(ρ), speed of sound(U), and viscosity(η) over entire compositions of 2MA(1)+2P(2), 3MA(1)+2P(2) and 4MA(1)+2P(2) with temperature ranges 303.15K, 308.15K, 313.15K, 318.15K and 323.15K are graphically illustrated in supplementary data. The occurrent feature of all these attributes as regards to mole fraction shows a non-linear increasing trend, and also shows reduction as regards to increasing temperature in entire compositions. The non-linear abnormalities of trends of these liquid components imply that molecular interactions exist between them.

The excess/deviation of thermodynamic acoustic parameters of a binary solution has been esteemed with several peer-reviewed journals. The eventual general expression was-

$$Y^E = Y^r - Y^{id} ----(1)$$

Here $Y^E = V_m^E, K_s^E, \Delta\eta$ and Y^r {=V_m(molar volume), K_s(isentropic compressibility) and η (viscosity)} is the real value of mixtures of the sample(1) and (2). And, the ideal component of thermodynamic acoustic parameters stands for,

$$Y^{id} = x_1 Y_1 + x_2 Y_2 ----(2)$$

x_1 and x_2 are the mole fractions of samples (1) and (2). And Y_1 and Y_2 are the parameter values of the pure values of individual components. The excess Gibb's energy of viscous flow can be evaluated from,

$$\Delta G^E = RT(\ln(\eta V) - (x_1 \ln(\eta_1 V_1) + x_2 \ln(\eta_2 V_2)) ----(3)$$

Redlich-Kister Polynomial Analysis

The inconsistencies in excess thermodynamic acoustic parameters for binary mixtures can be eliminated with a non-linear treatment of Redlich Kister polynomial regression[11].

$$Y^E = x_1 x_2 \Sigma_{p=0}^{p=N} A_{p,T}(x_1 - x_2)^p ----(4)$$

The standard deviation for excess thermodynamic acoustic parameters can be evaluated as follows-

$$\sigma(Y^E) = \sqrt{\Sigma_{i=1}^{i=N} \frac{(Y_{i,exp} - Y_{i,cal})^2}{M - N}} ----(5)$$

Where M stands for the number of experimental values and N stands for the adjustable parameter. These excess values are examined with Redlich-Kister polynomial non-linear regression, and the values of $A_{i,T}$ (i=0,1,2,3) are determined along with the standard deviation for experimental values and calibrated values. Table 3 cataloged the whole values of all composites.

The abnormality of thermodynamic acoustic excess parameters above is portrayed in Fig.-1, Fig.-2, Fig.-3 and Fig.-4 respectively. Due to thermal agitations of all composites, temperature rise ushers to descend

the excess parameters. The abnormality of (V_m^E) at all temperatures has been illustrated in Figure.1 over an entire concentration for all composites. The (V_m^E) values are attributes positive for high concentrations of 2P and the trend turns to negative during the increasing concentration of 2MA, 3MA and 4MA in the respective composites.

Table-3: Coefficients of Redlich-Kister Equation and Standard Deviations For Excess/Deviation Parameters of Various Binary Mixtures

System	*T/K*	Redlich Equation Coefficients				Error
		$A_{0,T}$	$A_{1,T}$	$A_{2,T}$	$A_{3,T}$	$\sigma(Y_{RK}^E)$
V_m^E (10^{-6} $m^3.mol^{-1}$)						
2MA+2P	303.15	0.0695	-4.6048	-2.8442	1.3835	0.0384
	308.15	0.0873	-4.4791	-2.8408	1.2441	0.0440
	313.15	-0.0078	-4.2507	-2.7566	1.7792	0.0112
	318.15	-0.0218	-3.2794	-2.213	1.4482	0.0307
	323.15	-0.0105	-3.0848	-2.1434	1.1983	0.0227
K_s^E (10^{-12} $m^2.N^{-1}$)						
2MA+2P	303.15	-0.0282	-0.0302	-0.0122	0.0119	$0.0783x10^{-06}$
	308.15	-0.0026	-0.0028	-0.0011	0.0011	$0.2111x10^{-06}$
	313.15	-0.0024	-0.0026	-0.001	0.001	$0.182x10^{-06}$
	318.15	-0.0022	-0.0024	-0.001	0.0009	$0.0018x10^{-06}$
	323.15	-0.002	-0.0022	-0.0009	0.0009	$0.0482x10^{-06}$
ΔG^E ($J.mol^{-1}$)						
2MA+2P	303.15	1325.02	-428.76	-28.55	1778.33	0.5709
	308.15	1394.08	-441.43	-0.94	1804.01	0.3521
	313.15	1558.46	-509.85	4.75	1906.97	0.0022
	318.15	1678.50	-550.62	-2.25	2003.43	0.1647
	323.15	1875.43	-649.19	12.40	2107.83	0.5714
$\Delta\eta$ (milli.Pa.sec)						
2MA+2P	303.15	-0.4309	0.2689	0.7719	1.8926	$1.5136x10^{-04}$
	308.15	-0.3743	0.2369	0.7231	1.7644	$1.2487x10^{-04}$
	313.15	-0.3238	0.2087	0.6904	1.6957	$1.5848x10^{-05}$
	318.15	-0.2954	0.1920	0.6444	1.6092	$1.2618x10^{-04}$
	323.15	-0.2641	0.1756	0.6315	1.5824	$1.0298x10^{-04}$
V_m^E (10^{-6} $m^3.mol^{-1}$)						
2MA+2P	303.15	-4.8363	-6.2468	6.9305	-1.6373	$6.3346x10^{-3}$
	308.15	-4.8123	-6.3945	6.8611	-1.4181	$7.4916x10^{-3}$
	313.15	-4.4967	-5.8894	6.1128	-1.0338	$9.8585x10^{-3}$
	318.15	-4.0815	-5.3589	5.4017	-0.8056	$2.2772x10^{-2}$
	323.15	-3.7806	-5.0268	5.0747	-0.5863	$1.1305x10^{-2}$
K_s^E (10^{-12} $m^2.N^{-1}$)						
3MA+2P	303.15	-0.0801	-0.0351	-0.0142	-0.0049	$0.1316X10^{-5}$
	308.15	-0.0744	-0.0333	-0.0137	-0.0047	$0.0821X10^{-5}$
	313.15	-0.0686	-0.0315	-0.0132	-0.0045	$0.0139X10^{-5}$
	318.15	-0.0629	-0.0292	-0.0124	-0.0043	$0.0276X10^{-5}$
	323.15	-0.0573	-0.0267	-0.0113	-0.0039	$0.0106X10^{-5}$
ΔG^E ($J.mol^{-1}$)						
3MA+2P	303.15	2136.78	-462.79	-668.67	1905.73	0.1263
	308.15	2164.27	-431.27	-701.02	1933.09	0.4336
	313.15	2223.30	-425.26	-761.40	1976.97	0.8570
	318.15	2306.59	-394.78	-870.12	2179.02	0.5506
	323.15	2447.90	-472.98	-850.39	2171.39	0.3572
$\Delta\eta$ (milli.Pa.sec)						
3MA+2P	303.15	0.4139	0.9541	-0.5588	1.7878	0.0053
	308.15	0.3438	0.8875	-0.5162	1.6085	0.0058

	313.15	0.2723	0.8293	-0.5245	1.3646	0.0071
	318.15	0.2467	0.8012	-0.4765	1.3577	0.0064
	323.15	0.2145	0.7191	-0.4299	1.2130	0.0060
V^E (10^{-6} m^3.mol^{-1})						
4MA+2P	303.15	-9.3765	0.0386	9.2487	-10.7508	0.2283
	308.15	-9.2805	0.0201	9.0549	-10.9126	0.2011
	313.15	-8.7024	0.8094	8.4195	-11.4936	0.1790
	318.15	-8.0820	0.8205	7.7922	-10.6268	0.1744
	323.15	-7.3608	0.6405	7.2201	-9.4606	0.1697
K_s^E (10^{-12} m^2 .N^{-1})						
4MA+2P	303.15	-0.1199	0	0.0263	0	0.2857X10-5
	308.15	-0.1115	0	0.0245	0	0.2685X10-5
	313.15	-0.1031	-0.0001	0.0226	0.0001	0.2584X10-5
	318.15	-0.0947	0	0.0207	0	0.266X10-5
	323.15	-0.0863	0	0.0189	0	0.2035X10-5
ΔG^E (J.mol^{-1})						
4MA+2P	303.15	2931.67	-2254.95	-1661.20	5570.80	6.0335
	308.15	3068.86	-2335.93	-1757.87	5777.04	5.9058
	313.15	3207.50	-2375.70	-1803.85	5796.67	4.1480
	318.15	3201.41	-2306.37	-1753.78	5623.97	3.8725
	323.15	3344.29	-2377.34	-1793.78	5699.42	2.5281
$\Delta\eta$ (milli.Pa.sec)						
4MA+2P	303.15	1.0171	-0.1333	-0.3830	4.7208	0.0194
	308.15	0.9409	-0.0905	-0.3609	4.3580	0.0166
	313.15	0.8395	-0.0537	-0.3276	3.8641	0.0137
	318.15	0.7198	-0.0328	-0.2870	3.3078	0.0111
	323.15	0.6507	-0.0322	-0.2556	3.0054	0.0103

The flipping sharpness of (V_m^E) from positive to negative was greater in 4MA(1)+2P(2) than compared to the other composites of 3MA(1)+2P(2) and 2MA(1)+2P(2) respectively. This clearly distinguishes the formation of H-bond, which is stronger at higher concentrations and weaker in lower concentrations of composites[12,13]. In addition to that, the formation of H-bond is very weak at high concentrations of 2P.

The (K_s^E) values are changed from high to low values for many composites. The sign of (K_s^E) plays a vital role in assessing the compactness due to molecular interactions in multi-component mixtures through electric charge transfer, dipole-dipole interactions, and dipole-induced dipole interactions in between bonds of successive constituent elements[14-16]. It also suggests interstitial accommodation and oriental ordering leading to more compact structure making, which enhances (K_s^E) negative values. Fort and Moore indicated that the binary liquids having distinct molecular sizes and shapes mix well thereby reducing the volume which causes values of (K_s^E) to be negative[17]. The flipping sharpness (K_s^E) of negative was greater in 4MA+2P than compared to the other composites of 3MA+2P and 2MA+2P respectively. This is visible in Figure.2, for the replicated sequence of (K_s^E) at any isolated temperature. This clearly distinguishes a greater steric hindrance to the formation of hydrogen bonds in the respective composites.

The (ΔG^E) values are attributes to positive for all composites. The sign (ΔG^E) leads to interactions of molecules through molecules energy. The positive values of (ΔG^E) distinguishing the existence of strong intermolecular interactions between the component molecules[14]. The sharpness of (ΔG^E) positive was greater in 4MA+2P than compared to the other composites of 3MA+2P and 2MA+2P respectively. This is visible in Fig.-3, for the replicated sequence (ΔG^E) of at any isolated temperature. The negative values of $\Delta\eta$ indicates mutual loss of dipolar association of molecules in composites, leads to bond formation between unlike molecules are relatively less than those of pure components[15]. This mainly attributes to the breaking of bonds ushers to weak dipole-dipole and dipole-induced dipole interactions, which are not sufficient to produce bulk entities in the composites. Contrary to the above, the positive

values of $\Delta\eta$ indicates a strong dipolar association of molecules in composites, leads to bond formation between unlike molecules are relatively greater than those of pure components. This mainly attributes to the strong dipole-dipole and dipole-induced dipole interactions, which are sufficient to produce bulk entities in the composites.

The formation of bulk entities is greater in 4MA+2P than compared to the other composites of 3MA+2P and 2MA+2P respectively. This is visible in Figure.4, for the replicated sequence of $\Delta\eta$ at any isolated temperature.

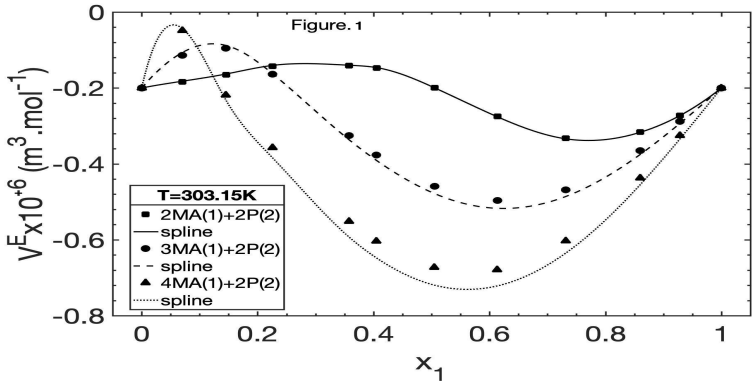

Fig.-1: Plot of Excess Volume Variations against Mole Fraction of Solutions ■2MA(1)+2P(2), ●3MA(1)+2P(2), ▲4MA(1)+2P(2) for the Isolated Temperature at 303.15K

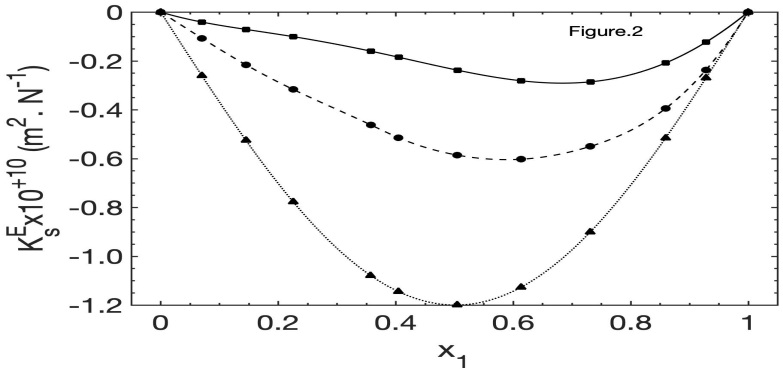

Fig.-2: Plot of Excess Isentropic compressibility Variations against Mole Fraction of Solutions ■2MA(1)+2P(2), ●3MA(1)+2P(2), ▲4MA(1)+2P(2) For the Isolated Temperature at 303.15K

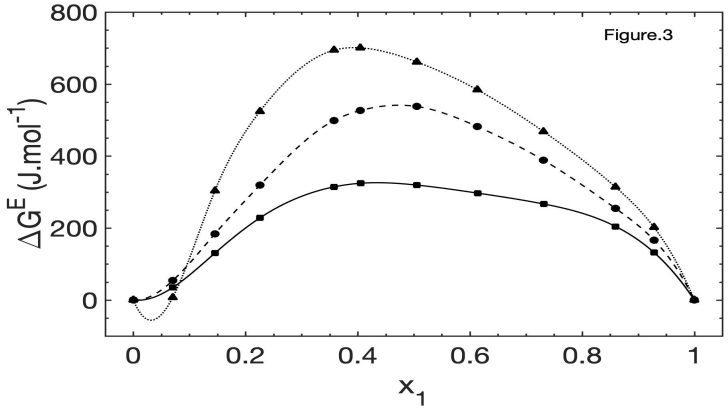

Fig.-3: Plot of Excess Gibbs Energy Function Variations against Mole Fraction of Solutions ■2MA(1)+2P(2), ●3MA(1)+2P(2), ▲4MA(1)+2P(2) for the Isolated Temperature at 303.15K

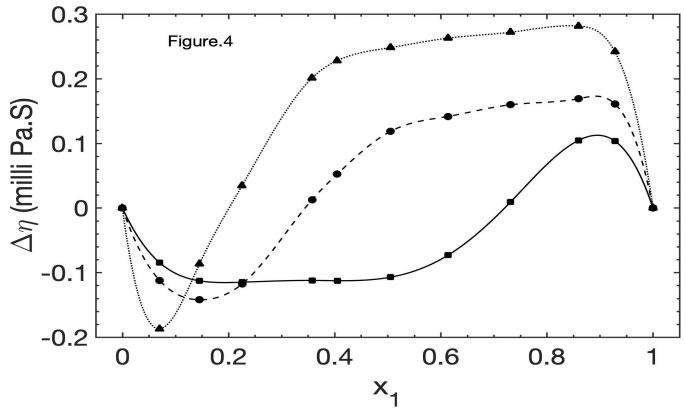

Fig.-4: Plot of Deviation in Viscosity Function Variations against Mole Fraction of Solutions ■2MA(1)+2P(2), ●3MA(1)+2P(2), ▲4MA(1)+2P(2) for the Isolated Temperature at 303.15K

Partial Molar Volumes

The Redlich-Kister equation can be expressed as-

$$A_{0,T} - A_{1,T} + A_{2,T} - A_{3,T} = \bar{V}^{E,\infty}_{1,p,m} = \bar{V}^{\infty}_{1,p,m} - V_{1,m} - - - -(6)$$

$$A_{0,T} + A_{1,T} + A_{2,T} + A_{3,T} = \bar{V}^{E,\infty}_{2,p,m} = \bar{V}^{\infty}_{2,p,m} - V_{2,m} - - - -(7)$$

$\bar{V}^{E,\infty}_{1,p,m}$ *and* $\bar{V}^{E,\infty}_{2,p,m}$ are excess partial molar volumes two pure components at infinite dilutions. $\bar{V}^{\infty}_{1,p,m}$ *and* $\bar{V}^{\infty}_{2,p,m}$ are partial molar volumes at infinite dilutions $V_{1,m}$ *and* $V_{2,m}$ are pure molar volumes of two components 2MA/3MA/4MA and 2P. But, the real-time analysis of partial molar volumes over a mole fraction concentration at constant pressure and temperature can be evaluated from the differential equation is-

$$\bar{V}_{i,p,m} = V_m(x_i) - x_j\left(\frac{\partial V_m(x_j)}{\partial x_j}\right)_{T,P} - - - -(8)$$

Here x_i and x_j are the mole fractions of two components in the composite (*i=1,2 and j=i-1*). The intermolecular interactions in the composites can be interpreted in terms of packing efficiency of molecules with the help of partial molar volumes.

The partial molar volumes of the two components $\bar{V}_{1,p,m}$ *and* $\bar{V}_{2,p,m}$ play a vital role in binary mixture[18]. Because the domain influence of the components in the mixture changes concerning the composition concentration and temperature. In this scenario, the partial molar volumes of components 2MA+2P, 3MA+2P and 4MA+2P at all temperatures have been shelled in Fig.-5a,b and c respectively. In each of the figures, the scaffolded Z symbol graph contains three colored meshes, which are concerned with green $\bar{V}_{1,p,m}$, brown (total molar volume, V_m) and magenta $\bar{V}_{2,p,m}$. For 4MA+2P combination, the partial molar volumes of both components $\bar{V}_{1,p,m}$ and $\bar{V}_{2,p,m}$ are higher than of the other two combinations of 3MA+2P and 2MA+2P. This reveals the domain influence of the individual components decreasing with their respective lower concentration regions. The abnormality is examined for all constant interval of temperatures. This suggests the presence of solute-solvent interactions in between unlike molecules[1]. Hence, from the representation of Fig.-5a,b and c, the effect of domain influence of volume is high for 4MA+2P. This suggests about, the solute-solvent interactions between molecules are high for 4MA+2P than compared to the other composites of 3MA+2P and 2MA+2P.

The new pertinent expression proposed by Belda, which correlates the total molar volumes with a factor to linearize the homographic function over a molar fraction of one component in binary mixture. The Belda expression as:[19]

$$Y_B(x_1) = Y_2 + (Y_1 - Y_2)x_1\frac{1 + m_1(1 - x_1)}{1 + m_2(1 - x_1)} - - - -(9)$$

Here m_1 and m_2, are two pertinent empirical adjustable parameters for all composites that can be evaluated from the non-linear regression analysis. Recently, several pioneers discussed the correctness of Belda

proposal and concluded that this equation can give preferable results than the RK one with the same number of free parameters. From the above expressions, the partial excess molar volumes at infinite dilutions can be easily obtained as:

$$\bar{V}^{E,\infty}_{1,p,m} = \bar{V}^{\infty}_{1,p,m} - V_{1,m} = \frac{m_1 - m_2}{1 + m_2}(V_{1,m} - V_{2,m}) - - - -(10)$$

$$\bar{V}^{E,\infty}_{2,p,m} = \bar{V}^{\infty}_{2,p,m} - V_{2,m} = (m_1 - m_2)(V_{1,m} - V_{2,m}) - - - -(11)$$

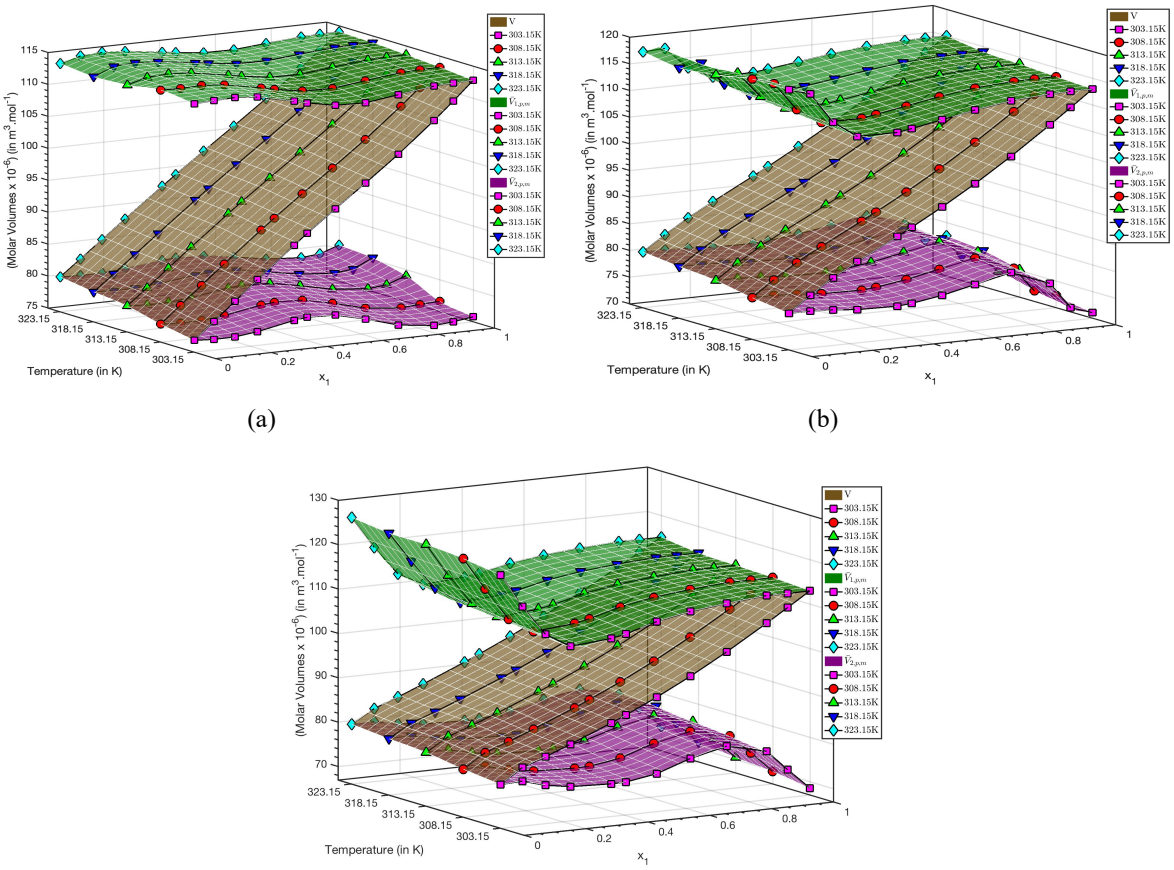

(a) (b)

(c)

Fig.-5: Plot of Mole Fraction Dependent on Partial Molar Volumes in the Solution of (a) 2MA(1)+2P(2) (b) 3MA(2)+2P(2) (c) 4MA(1)+2P(2) at studied Range of Various Temperatures (303.15K -323.15K).

Table-4: Comparison Table For Extrapolation Values with Belda theory equations

	T/K	m_1	m_2	$\sigma_Y(B)$	Extrapolation		Belda	
					$\bar{V}^{E,\infty}_{1,p,m}$	$\bar{V}^{E,\infty}_{2,p,m}$	$\bar{V}^{E,\infty}_{1,p,m}$	$\bar{V}^{E,\infty}_{2,p,m}$
2MA+2P	303.15	-23.5113	-23.3183	0.6893	0.3095	-6.9392	0.3109	-6.9392
	308.15	-17.5778	-17.4058	0.9517	0.3696	-6.1011	0.3719	-6.1012
	313.15	23.7435	23.8955	0.2733	-0.2120	-5.2557	-0.2111	-5.2557
	318.15	7.3025	7.4266	0.2343	-0.5107	′-4.2520	-0.5046	-4.2520
	323.15	12.1135	12.2360	0.7007	-0.3132	-4.1138	-0.3108	-4.1138
3MA+2P	303.15	-1.6860	-1.6863	1.0354	10.5272	-6.1031	9.6199	-5.9336
	308.15	-1.7130	-1.7147	0.9824	9.8780	-5.7076	8.9587	-5.5418
	313.15	-1.6796	-1.6787	0.8860	8.4846	-5.1816	8.2945	-5.1484
	318.15	-1.7120	-1.7126	0.8292	7.4240	-4.7005	7.6214	-4.7367
	323.15	-1.7022	-1.7024	0.7490	6.9489	-4.3199	6.9443	-4.3173
4MA+2P	303.15	-2.3847	-2.0475	86.0983	11.7470	-12.1878	11.6348	-12.1878
	308.15	-2.3804	-2.0637	62.2683	11.1709	-11.6595	10.6253	-11.3025

	313.15	-2.3823	-2.0667	87.9378	10.4656	-10.9539	10.2694	-10.9539
	318.15	-2.4433	-2.0879	60.4703	9.6892	-10.1532	11.2285	-12.2153
	323.15	-2.3994	-2.1036	37.2248	8.8272	-9.2120	9.2894	-10.2517

FT-IR Spectrum Analysis

The FT-IR spectrum of all combinations and their pure components are carried at room temperature 303.15K[20]. The peaks of the intensity of N-H stretching sharp primary peak and N-H stretching sharp secondary peak are simply turn in to O-H stretching broad peak for the combination of 4MA+2P. That means, strong H-bond interactions occurring in 4MA+2P than the rest of the other two combinations. The C-H stretching medium peaks, C-N stretching sharp peaks and C-H bending sharp peaks are most effective in 4MA+2P than the rest of other combinations. This is illustrated in Table-5 and Fig.-6. Hence, the combination of 4MA+2P is stronger than 3MA+2P and 2MA+2P. This contention was supported by the formation of intermolecular strong bonds.

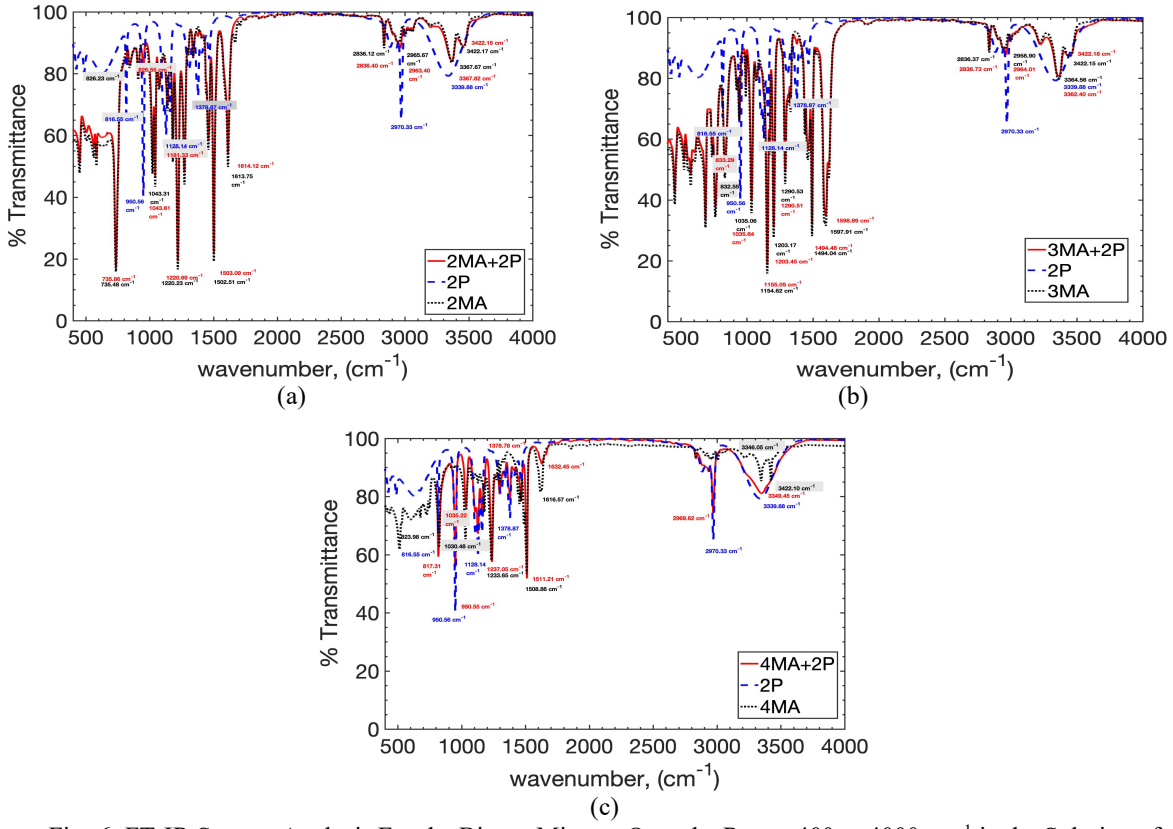

Fig.-6: FT-IR Spectra Analysis For the Binary Mixture Over the Range 400 to 4000 cm^{-1} in the Solution of (a) 2MA(1)+2P(2) (b) 3MA(2)+2P(2) (c) 4MA(1)+2P(2) at studied Range of Various Temperatures (303.15K - 323.15K).

Table-5: FTIR Analysis

Name of the Component	N-H Stretching Secondary cm^{-1}	N-H Stretching Primary cm^{-1}	C-H Stretching Medium cm^{-1}	C-N Stretching cm^{-1}	O-H Stretching (H-bonded) cm^{-1}	C-H Bending cm^{-1}
2MA	3422.17	3367.67	2965.67	1220.23	--	826.55
2MA+2P	3422.15	3367.82	2963.40	1220.69	--	826.23
3MA	3422.15	3364.56	2958.90	1203.17	--	832.55
3MA+2P	3422.18	3362.40	2964.01	1203.45	--	833.29
4MA	3422.10	3346.05	2965.67	1233.65	--	823.98
4MA+2P	--	--	2963.40	1233.65	3349.45	817.31
2P	--	--	2970.33	--	3339.88	816.55

CONCLUSION

In this framework, the values of excess thermodynamic parameters have been calibrated for entire compositions of 2MA(1)+2P(2), 3MA(1)+2P(2) and 4MA(1)+2P(2) with accustomed levels of temperatures. This is elucidating a strong hydrogen bonding, dipole-inclusion interactions present in the component molecules. The reactive of composites are in the order of 2MA(1)+2P(2) < 3MA(1)+2P(2) < 4MA(1)+2P(2). In this connection, the partial molar volumes of both components have been plotted in 3D graphs. This discloses the intermolecular interactions are strong in 4MA+2P composition compared to 3MA+2P and 2MA+2P. This result of intermolecular interaction behavior is also supported by FT-IR spectroscopy.

ACKNOWLEDGEMENT

One of the authors (Dr. Shaik.Babu) would like to thank the Department of Science and Technology (DST), Govt. of India, for the award of the DST-FIST Level-1 (SR/FST/PS-1/2018/35) scheme to the Department of Physics, KLEF. Author, G V Gangadhara Rao is thankful to Dr. Shaik Babu, Department of Physics, KLEF, Guntur for his valuable suggestions and discussions.

REFERENCES

1. S. S. Sastry, S. Babu,T. Vishwam, H. Sie Tiong. *Journal of Chemical Thermodynamics,* **68**, 183 (2014), **DOI:**10.1016/j.jct.2013.09.005
2. S. S. Sastry, S. Babu,T. Vishwam, H. Sie Tiong. *Journal of Thermal Analysis and Calorimetry,* **116**, 923(2014), **DOI:**10.1007/s10973-013-3570-9
3. K.G. Rao, Kiran M. Gnana Kiran, S. Babu, D. Santos, *Journal of Pharmaceutical Sciences and Research*, **9,** 624(2017).
4. T. Kalimulla, S. Babu, D. Das, M. Gowrisankar, K.G. Rao, *Journal of Pharmaceutical Sciences and Research*, **11**, 2645(2019).
5. T. Kalimulla, A. Nagurjuna, S. babu, K. G. Rao, *Asian Journal of Chemistry,* **30**, 2008(2018), **DOI:**10.14233/ajchem.2018.21385
6. S. S. Sastry, S. Babu, T. Vishwam, K. Parvateesam, H. Sie Tiong, *Physica B: Condensed Matter,* **420,** 40(2017), **DOI:**10.1016/j.physb.2013.03.028
7. N. Haldar, H.S. Shukla, G. Udayabhanu, *Indian Journal of Chemical Technology,* **19,** 173(2012).
8. T. Kalimulla, D. Das, M. Gowrisankar, K.G. Rao, S. Babu, *Rasayan Journal of Chemistry,* J **12,** 1909(2019), **DOI:**10.31788/RJC.2019.1245481
9. S. Shihab, S. Babu, S.S. Sastry, *Rasayan Journal of Chemistry,* **9**, 641(2014).
10. K.G. Rao, S.Babu, *Rasayan Journal of Chemistry*, **12**, 1110(2014), **DOI:**10.1007/s10973-013-3570-9
11. O. Redlich, A.T. Kister, *Industrial and Engineering Chemistry,* **40**, 345(1948), **DOI:**10.1021/ie50458a036
12. R.L. Gardas, D.H. Dagade, S.S. Terdale, J.A.P Coutinho, K.J. Patil, *The Journal of Chemical Thermodynamics,* **40**, 695(2008), **DOI:**10.1016/j.jct.2007.10.007
13. S.L. Oswal, R.L. Gardas, R.P Phalak, *Journal of Molecular Liquids,* **116**, 109(2005), **DOI:**10.1016/j.molliq.2004.07.081
14. A. Pal, H. Kumar, B. Kumar, R. Gaba, *Journal of Molecular Liquids*, **187**, 278(2013), **DOI:**10.1016/j.molliq.2013.08.009
15. B. Mukesh, M. G. Sankar, M. C. Shekar, T. Srikanth, *Journal of Solution Chemistry,* **44**, 2267 (2015), **DOI:**10.1007/s10953-015-0406-1
16. T. Vishwam, K. Parvateesam, S. Babu, S.S. Sastry, V.R.K. Murthy, *Indian Journal of Pure and Applied Physics,* **54**, 597(2016)
17. R.J. Fort, W.R. Moore, *Transactions of Faraday Society,* **67**, 2102(1971).
18. D. Das, A. Messaadi, N. Dhouibi, N. Ouerfelli, *Physics and Chemistry of Liquids,* **50**, 773(2012), **DOI:**10.1007/BF02767781
19. S. P. Sulthana, M. Gowrisankar, S. Babu, D. Santos, *International Journal of Ambient Energy*, 1(2019), **DOI:**10.1080/01430750.2019.1673816
20. P. Suneetha, T.S. Krishna, M. Gowrisankar, D. Ramachandran, *Journal of Molecular Liquids,* **238**, 170 (2017), **DOI:**10.1016/j.molliq.2017.04.129

[RJC-5825/2020]